Vol. 20, No. 3(2021) Bio2390
Revista Mexicana de Ingeniería Química

Microbial electrochemical system for obtaining value-added products using a halotolerant bioanode

Sistema electroquímico microbiano para la obtención de productos de valor agregado utilizando un bioanodo halotolerante

E. González, B. Escobar-Morales, R. Tapia-Tussell, L. Alzate-Gaviria*,

Renewable Energy Unit, Yucatan Center for Scientist Research, Mérida, CP 97302, Mexico.

Received: February 28, 2021; Accepted: September 14, 2021

Abstract

Microbial electrochemical systems (MES) cathodic reaction have stood out in the last decade, due to their versatility for the production of several chemical products of commercial interest using renewable energy. This work addresses the use of halotolerant microorganisms as bio-anodes with saline electrolytes (50 gL^{-1} NaCl), with a lower resistance and energy loss compared to freshwater systems. Likewise, it was demonstrated that it is possible to recover lanthanide in the form of oxides from a highly saline electrolyte. Being the first work in the literature to report the recovery of this metal from an aqueous solution in MES, opening a door for the development of MES specialized in the recovery of rare earth elements.

Keywords: microbial electrochemical systems, material recovery, halotolerant bioanodes.

Resumen

La reacción catódica de los sistemas electroquímicos microbianos (MES) se ha destacado en la última década, por su versatilidad para la producción de diversos productos químicos de interés comercial utilizando energías renovables. Este trabajo aborda el uso de microorganismos halotolerantes como bioanodos y electrolitos salinos (50 gL^{-1} NaCl), con una menor resistencia y pérdida de energía en comparación con los sistemas de agua dulce. Asimismo, se demostró que es posible recuperar lantánidos en forma de óxidos a partir de un electrolito altamente salino. Siendo el primer trabajo en la literatura en reportar la recuperación de este metal a partir de una solución acuosa en MES, abriendo una puerta para el desarrollo de MES especializados en la recuperación de elementos de tierras raras.

Palabras clave: sistemas electroquímicos microbianos, recuperación de materiales, bioanodos halotolerantes.

* *Corresponding author. E-mail*: lag@cicy.mx
https://doi.org/10.24275/rmiq/Bio2390
ISSN:1665-2738, *issn-e*: 2395-8472

1 Introduction

Microbial electrochemical systems (MES) are electrochemical devices where microorganisms are used as catalyst. Usually, microorganisms supported on an electrode are used as bioanode in order to harvest an electric current coupled to organic matter removal from the electrolyte (Gómora-Hernández *et al*., 2020).

The electrosynthesis of chemicals, contaminants removal, biosensor development, and substances recovery include hydrogen production for fuel, also different organic acids and valuable metals such as copper, cobalt, cadmium, zinc, gold, and silver, among others (Kadier *et al*., 2020; Hua *et al*., 2019; Zhang and Angelidaki, 2014).

The demand of valuable metals is rising, and suddenly the land reserves are insufficient to supply the future demand. As a solution, alternative sources of metals must been taken into advantage, like wastewaters, industrial and urban waste leachates, or extreme environments such as the oceanic floor, placers or geothermal brines. Despite that mature technologies for metal recovery such as pyrometallurgical and hydrometallurgical methods are already available, these are not suitable to perform the extraction from diluted matrixes, are high energy consuming, produce harmful gases, and are not environmentally friendly as large amounts of solvents and chemicals are required. Many of these problems can be overcame with MES technologies as they are suitable for metal recovery from diluted aqueous solutions, consume low amounts of energy (less than 2V) where the most part is renewable, are environmentally friendly, and the cathode reaction and operational conditions are adjustable to separate some metals from complex mixtures (Jordens *et al*., 2013; Jha *et al*., 2016; Xie *et al*., 2014).

However, it has been demonstrated that halotolerant bioanodes allow increasing the salinity of the electrolyte in order to decrease the internal resistance of the system, without causing any impairment to microbial activity. Also, high salt concentration in the electrolyte help to avoid contamination with microorganisms from the environment and to maintain a low dissolved oxygen concentration, since sterile or anaerobic conditions are not required for its handling (Reimers *et al*., 2006, 2007).

On the other hand, rare earth elements (REEs) are considered critical raw materials of economic importance and technological value (renewable energy technologies as eolic turbines, photovoltaic cells, energy storage, catalysts for oxygen and hydrogen evolution, electric cars; medical imaging, visual displays in screens and low energy lighting, among many others), but also to its high-risk of supply interruptions (Dehaine *et al*., 2015; Massari and Ruberti, 2013; Morrison and Tang, 2012).

REEs have a reduction potential which is far beyond water stability limits (E° = -2.6 V/SHE). At this potential, the hydrogen evolution reaction exceeds the elemental reduction reaction of metals, hindering metal precipitation. Interestingly, the recovery of solid cerium hydroxides and oxides from aqueous solutions has been extensively reported in the literature since many decades ago to the date, either by alkaline or electrochemical precipitation, mainly for cerium nanoparticle production or in order to obtain cerium powders and composites with catalytic properties. Despite all this evidence, the recovery of REE in MES has not been studied yet.

The aim of this study is to demonstrate that it is possible to recover a REE as oxides by cathodic recovery from a diluted aqueous solution in a MES, operating with a halotolerant bioanode at high salt concentrations. Cerium was the element chosen to conduct this work, due to its abundance and multiple applications, but above all because it is a common reported REE in the literature regarding alkaline precipitation.

2 Materials and methods

2.1 *Development of halotolerant microbial bioanodes*

Three prefabricated ambar crystal cells were employed (180 mL of useful volume) to set a three electrode system. The halotolerant bioanode was supported on carbon felt (projected area of 7 cm^2) with a platinum wire as collector (working electrode). A graphite rod (projected area of 17.25 cm^2) was used as counter electrode and standard saturated calomel electrode as reference (+0.241 V/SHE). The distance among all electrodes was of 3 cm. The chamber was filled with culture medium (pH = 7.9) supplemented with NaCl (50 g L^{-1}) and sodium acetate (3.6 g L^{-1}) as carbon source (Prakash *et al*., 2010). Sediments collected from an hyperhaline lagoon (“Ría Lagartos", at Las Coloradas, Yucatán, México) were used as inoculum

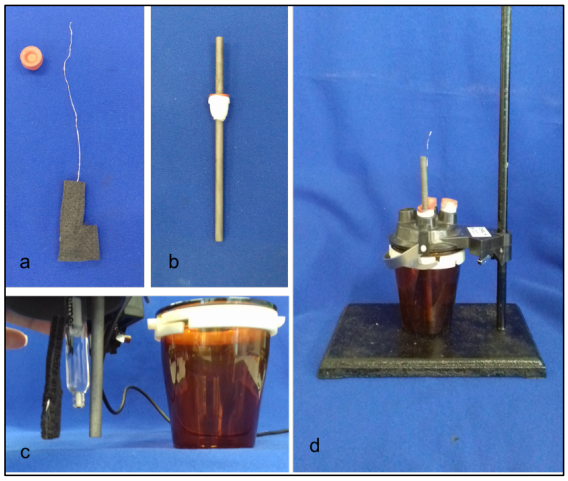

Figure 1. Development of halotolerant microbial bioanodes; a) Carbon felt anode with Pt wire as collector, b) graphite cathode, c) electrode configuration, d) cell side view.

(15% v/v). The salinity of the collection site was 50 g L^{-1} as described elsewhere. A chronoamperometry at -0.16 V/SHE was performed during 21 days with a BioLogic VSP 400 potentiostat in order to develop the bioanodes (Kumar 2019; Prakash *et al*., 2010).

2.2 *MES start-up (bioanode adaptation)*

A cylindrical two-chamber MES was made in acrylic (450 mL total volume, each), separated with a proton exchange membrane (70 cm^2 - Nafion® 117), activated as Prakash *et al*. (2010). Each chamber had sampling and feeding ports, as well as for placing reference electrodes.

A halotolerant bioanode was placed in the anode chamber of the MES and used as working electrode, a graphite rod (projected area of 17.25 cm^2) was used as counter electrode, and a Ag/AgCl electrode as reference (+0.197 V/SHE). The electrodes were separated less than 1 cm between each one. The anode chamber was filled with fresh culture media and re-inoculated with 15% v/v of fresh sediments. The cathode chamber was filled with saline solution and remained disabled (NaCl 50 g L^{-1}, pH = 7.9) A chronoamperometry was conducted at -0.160 V/SHE over three weeks, until current production was stable and open circuit anodic potential reached values near the acetate oxidation potential (-0.298 V/SHE), indicating that the acetate-dependent exoelectrogenic microbial community supported on the bioanode was well adapted to the MES (Peeva *et al*., 2020; Morrison and Tang, 2012; Ter Heijne *et al*., 2006).

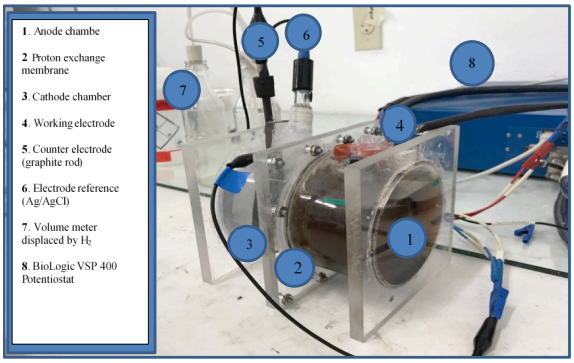

Figure 2. Microbial electrochemical systems start-up.

Carbon source depletion was monitored by Chemical Oxygen Demand (COD Low Range Hach-Lange Kit) and replenished every three to five days. Dissolved oxygen, conductivity and pH were periodically measured with Hach-Lange portable electrodes.

2.3 *MES configuration for cerium oxide recovery*

After the MES start-up, a 304 stainless steel plate was placed in the cathodic chamber and used as working electrode (2 cm^2 of projected area) at 2 cm from an Ag/AgCl electrode, used as reference (+0.197 V/SHE). The cathodic chamber was filled with a NaCl (50 g L^{-1}) solution, and $CeCl_3 \cdot 7H_2O$ (0.42 g Ce L^{-1}) as analyte for cathodic cerium recovery. The bioanode remained in the anodic chamber, but this time was used as counter electrode. The distance between the anode and the cathode was 8 cm.

The cerium oxide recovery reaction was conducted by chronopotentiometry at -2.5 Am^{-2} for 48 h, by triplicate. Prior to each reaction, the anode chamber was filled with fresh culture media (pH = 7.9) and also the catholyte in the cathode chamber was renewed. The experiment was conducted under batch feeding regime. During the reaction, the close circuit cell potential was measured with a Fluke 179 multimeter. Catholyte pH values were measured at 0 h, 24 h and 48 h, and anolyte pH values at 0 h and 48 h. After every reaction, the working electrode was disconnected and withdrawn from the cathodic chamber and stored for its further characterization. The catholyte was removed carefully with a syringe, to avoid disturbing the precipitate settled at the bottom of the cathodic chamber. The precipitate was also recovered and reserved for characterization.

A fourth reaction was performed in the MES as control, with a bioanode starved until death (no

exoelectrogenic activity detected). Also, as additional controls, the cerium oxide recovery was characterized by chronopotentiometry (-2.5 A m^{-2} for 48 h, by triplicate) in abiotic conditions using a three-electrode set-up performed in a crystal prefabricated electrochemical cell filled with 180 ml of the catholyte solution. A 304 stainless steel plate (2 cm^2 of projected area) was used as working electrode, a DSA mesh (De Nora, 10 cm^2 as projected area) as counter electrode, and a SCE as reference, separated by a 3 cm distance.

2.4 Cerium oxide characterization

The cathode was dried at 105 °C for 24 h to remove the excess of water. The amount of recovered material on the cathode surface was estimated by weight difference. The material was scraped with a spatula and analyzed by X Ray diffraction (XRD). On the other hand, the precipitates recovered from the bottom of the cathode chamber were centrifuged (8,000 rpm, 10 min) and the pellets were dried at 105 °C for 5 days. The resulted powder was analyzed by XRD. The XRD patterns were obtained with an X Ray Bruker D-8 diffractometer using Cu-Kα radiation at a scan rate of 0.02° s^{-1}, within a 2θ interval of 10 to 100°. Also, the recovered material was analyzed by SEM-EDS (Scanning Electron Microscope-Energy Dispersive X-ray Spectrometer) to determine its elemental composition.

2.5 Statistical analysis

For comparisons between some data an analysis of variance was performed between data sets with an α = 0.05 (Minitab 17 Software).

3 Results and discussion

3.1 Halotolerant bioanode growth

Current density production was observed at a negative potential (-0.16 V/SHE) after two or three days of polarization. This is in agreement with the results of Torres *et al*. (2009) and Gaffney *et al*. 2021, who observed a faster start-up at lower potentials when marine sediments were used as inoculum. Maximum current density peaks were reached after 16 days of polarization. The highest values registered was 2.5 A m^{-2}. This was consistent with results reported by Zhu *et al*. (2014) and Rimboud *et al*. (2021).

3.2 Cerium oxide recovery in the MES

The cathode potential decreased abruptly at the beginning of each reaction from +0.060 ± 0.036 V/SHE to -0.881 ± 0.05 V/SHE, and remained stable for the rest of the experiment. During the reaction, a white precipitate appeared on the electrode surface and its surroundings right after the hydrogen evolution in the cathodic chamber was observable. The pH value at the beginning of the reaction (0 h) was 5.22 ± 0.45, which increased by about two units after 24 h of chronopotentiometry, reaching 7.37 ± 0.31 units. These observations were consistent with abiotic controls, where initial pH was 4.16 ± 0.35 and raised about two units at the middle of the reaction (24 h). The increment in pH during the cathodic reaction is expected, as reported by Zhou and Switzer (1996), who obtained cerium oxide powder by electrochemical generation of hydroxyl ions. This process implies, first, hydrogen evolution from hydronium ion discharge on the electrode metal surface in acidic conditions (Eq. 1) followed by Heyrovsky step (Eq. 2) or Tafel recombination (Eq. 3), and secondly, water discharge on the metal surface (Eq. 4), which led to hydroxyl ion generation (Stamenkovic *et al*., 2017; Fraggedakis and Bazant 2020):

$$H_3O^+ + M + e^- \leftrightarrow M - H^*_{ads} + H_2O \quad (1)$$

$$H_3O^+ + M - H^*_{ads} + e^- \leftrightarrow M + H_2 + H_2O \quad (2)$$

$$2M - H^*_{ads} \leftrightarrow 2M + H_2 \quad (3)$$

$$H_2O + e^- + M \leftrightarrow M - H^*_{ads} + OH^- \quad (4)$$

On the other hand, hydroxyl groups could be generated by oxygen reduction reaction at the cathode (Stamenkovic *et al*., 2017) as it is shown in Eq. 5, which has a standard reduction potential of +0.401 V/SHE:

$$O_2 + 2H_2O + 4e^- \leftrightarrow 4OH^- \quad (5)$$

At the end of the cathodic reaction pH values remained neutral (7.06 ± 0.61) meanwhile they returned to acidic values in the abiotic controls (4.15 ± 0.21). The phenomenon observed in the controls is due to the hydroxyl ions being consumed for the formation of cerium hydroxides (Eq. 6) and the concomitant generation of hydronium ions by cerium hydroxide oxidation to cerium oxide (Eq. 7) (Zhou and Switzer,

1996; Wang *et al*., 2016).

$$Ce^{+3} + yOH^{-} \rightarrow Ce(OH)_{y}^{(3-y)} \quad (6)$$

$$Ce(H_2O)_x(OH)_{y}^{(4-y)+} + H_2O \rightarrow CeO_2 \cdot nH_2O + H_3O^{+} \quad (7)$$

In contrast, the experiments performed in the MES showed neutral pH values at the end of the reaction because of the migration of hydronium ions through the proton exchange membrane to the anodic chamber, supported by the fact that anodic pH decrease from 8.03 ± 0.20a to 7.60 ± 0.22b (Pikalova *et al*., 2021; Zhou and Switzer, 1996).

The cell potential needed to sustain the current -2.5 A m^{-2} was between 0.62 and 1.00 V. Interestingly, the cell potential incremented gradually with each reaction. In detail, cell potential was between 0.620 to 0.680 V in the first reaction, between 0.640 to 0.720 V in the second reaction and 0.780 to 1.000 V in the third. The cell voltages registered during the three reactions were lower in comparison with the fourth reaction used as control, where 1.7 V were needed to sustain the cathodic reaction in absence of exoelectrogenic activity (MES control). Cell potential values in the first and second reaction were similar to those reported by Wang *et al*. (2016), who recovered Cd by reduction to its elemental form (E = -0.520 V/EEH) on a SEM cathode (0.500 y 0.700 V). However, the cathodic potential recorded by Wang *et al*. (2016), was higher (-0.776 to -0.621 V/EEH) in comparison with this work (-0.881 ± 0.05 V/SHE). In general, the cell voltage applied to recover metals as Cu, Cd, Pb, Zn, among others, in MES is about 0.5 and 1.7 V according to several reports (Jin and Zhang, 2020; Wang *et al*., 2016; Luo *et al*., 2014; Modin *et al*., 2012).

3.3 *Characterization of Cerium oxide deposit in a MES configuration*

A total mass of 94.70 ± 4.21 mg from the bottom of the cathodic chamber and 8.77 ± 1.55 mg of material was recovered on the cathode surface (Figure 3a and b). After the drying process the material presented a white yellowish color. XRD patterns revealed the presence of CeO_2 (ceranite COD-Inorg 96-900-9009) and NaCl (halite COD-Inorg 96-434-3162) in the crystalline fraction of all the samples; a representative pattern is shown in Figure 4.

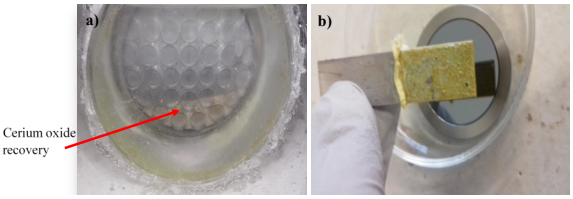

Figure 3. Material recovered; a) Bottom side of the cathodic chamber, b) On the cathode surface.

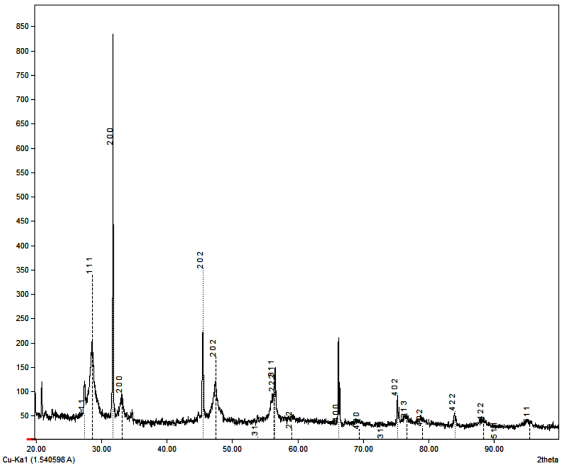

Figure 4. X-ray diffractogram performed on the deposits obtained in the SEM cathode. Dashed line: CeO_2 diffraction pattern [COD-Inorg 96-900-9009]. Dotted line: NaCl diffraction pattern [COD-Inorg 96-434-3162].

The elemental composition of the samples calculated by SEM-EDS is shown in Table 1, being cerium the most abundant element on the samples (>50%), followed by oxygen, sodium and chlorine. The results were consistent with the XRD patterns.

Based on EDS results, the total amount of cerium recovered in the samples was calculated. 103.47 ± 5.75 mg of material were recovered, both, from the surface of the cathode and from the bottom of the cathodic chamber, of which 53.02 ± 3.39 mg were corresponded to Ce. This represents a total recovery of 28.34 % of the dissolved Ce, where 8.28 ± 1.48 % was recovered on the electrode surface and 93.56 ± 7.22 % on the bottom of the cathode chamber.

The total Ce recovery (28.34 ± 1.81 %) was less than the percentage of Cd recovered by Wang *et al*. in a MES, which was up to 46.6 ± 1.3 %, consuming between 0.5 - 0.7 V. In this work the amount of Ce was recovered exclusively by hydroxyl ion generation, in comparison to Wang *et al*. (2016), where Cd was recovered mainly by direct electrochemical reduction to its elemental form.

Table 1. Elemental composition of Ce deposits obtained by SEM-EDS under brackish conditions.

Element	Material recovered on the electrode surface	Material recovered from the bottom of the cathodic chamber
Ce	50.11 ± 1.30%a	52.39 ± 3.30%a
O	24.34 ± 0.84%a	25.38 ± 2.22%a
Na	12.94 ± 1.26%a	11.57 ± 2.96%a
Cl	12.61 ± 0.07%a	10.66 ± 2.34%a

They reported a recovery rate of 5.27 mg L^{-1} h^{-1}, which was superior than 2.43 mg L^{-1} h^{-1} reported here. This is presumably due to the feeding regime, as Wang *et al*. (2016), used a continuous system in comparison with this work, where the system was fed in a batch regime.

In another work, Luo *et al*. (2014), used a MES for Cu, Ni and Zn recovery, applying a voltage of 1.0 V to the circuit of the microbial electrolysis cells reactor. After 48 h of operation the metal recovery achieved between 45 and 95 %, being this value inversely proportional to the standard reduction potential of each metal to its elemental form (+0.342 V/SHE Cu, -0.257 V/SHE Ni y -0.447 V/SHE Fe) (Vanýsek, 2012), explaining why the cerium percentage recovery reported here is lower in comparison to other reports (-2.34 V/SHE Ce) (Vanýsek, 2012), as no elemental reduction of the metal occurs for Ce at the recorded cathodic potential (-0.881 ± 0.05 V/SHE). The same phenomenon was reported by Modin *et al*. (2012), in a MES for Cu, Pb, Cd and Zn recovery, achieving between 44 and 84 % of recovery, employing between 0.34 and 1.70 V to sustain the reaction. Interestingly, Luo *et al*. (2014), report a Cu and Ni reduction to its elemental form, meanwhile Fe was recovered as oxides, indicating that at lower standard reduction potentials to elemental form, the metal recovery as hydroxides and oxides is more prone to occur by the hydroxyl ions produced at the cathode, and the percentage of metal recovered at its elemental form is lower. Taking this into account, it is not surprisingly that elements like Cu, Ni and Fe are recovered by both mechanisms (elemental form and precipitation by hydroxyl ions), which is not possible for cerium recovery as its standard reduction potential is far beyond the stability limits of water, making the precipitation by hydroxyl ions the only way to recover this element in aqueous solution in MES with an abiotic cathode (Luo *et al*., 2014; Modin *et al*., 2012).

Pozo *et al*. (2017), employed an electrochemical electrolysis cell to generate hydroxyl ions at the cathode to recover dissolved metals from acid mine drainage. They recirculated the mine drainage from a 1.7 L reactor to a 300 mL cathodic chamber; sulfur was employed as electron donor at the anode. They applied 1.7 V to obtain a current density of 4.5 A m^{-2}, and recovered 100% of Al, Zn, Cu, As and Cr, and 91 to 99 % of Fe, Mg, Mn, Ni, Co, Pb and Cd, in 17 h of operation. During the process the pH incremented from 2.7 to 7.3. Interestingly, the metal recovery decrease 50 % when the cell was operated in batch mode, indicating that the results obtained in this work may be improved in a continuous regime. Even if the cerium recovery percentage in our work (28.34 ± 1.81%) was lower than the percentages reported by Pozo *et al*. (2017), the cerium recovery rate reported here (2.43 mg L^{-1} h^{-1}) was in the range reported by Pozo *et al*. (2017), which was between 1.92 and 7.46 mg L^{-1} h^{-1}. The authors also reported an REE and Yttrium recovery but the values were not published.

On the other hand, when the EDS and XRD results were compared, a discrepancy was observed in terms of mass balance if only CeO_2 and NaCl are considered as the chemical species in the product. The percentage composition of CeO_2 correspond to 81.41 % of Ce and 18.59 % of O, while NaCl is composed of 39.66 % Na and 60.34 % Cl. In contrast, the composition showed by the EDS was 67.30 ± 1.26 % of Ce and 32.70 ± 1.26 % of O in the material recovered on the plate, and 67.38 ± 1.18 % and 32.62 ± 1.18 %, respectively, in the precipitate obtained at the bottom of the cathode chamber. The same situation was observed for the NaCl, finding that the composition of the product was 50.60 ± 1.59 % Na and 49.40 ± 1.59 % Cl on the plate and 51.87 ± 1.88 % Na and 48.13 ± 1.88 % Cl in the precipitate. This indicates that a redundant of O and Na were present of both products.

The scanning electron microscopies performed on the samples of the deposits recovered on the electrode, as well as precipitates in the electrolyte, are shown

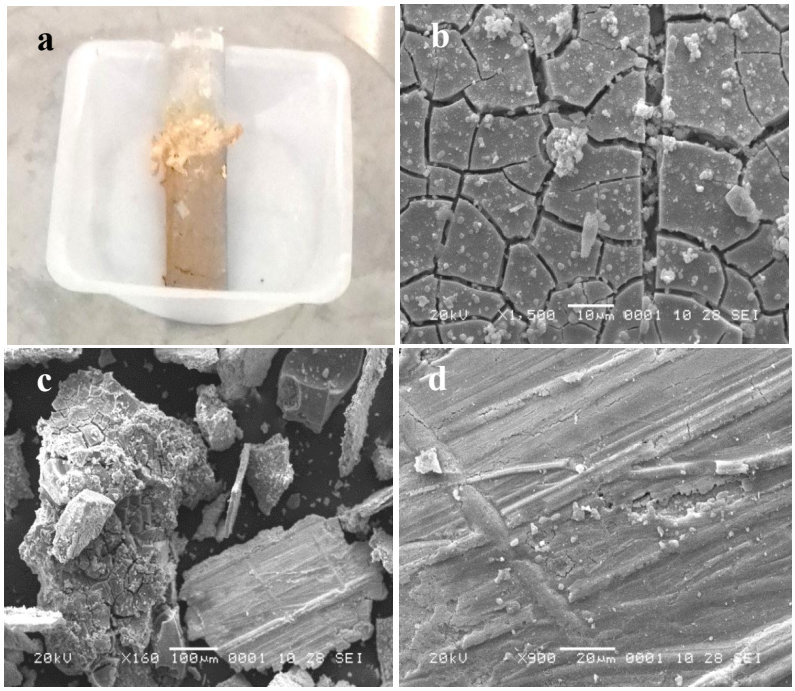

Figure 5. Magnification SEM images of cerium deposits (CeO_2) on the MES cathode under brackish conditions. a: Deposit obtained on a stainless steel electrode; b: 24 hours; c and d: 48 hours obtained by electrochemical generation.

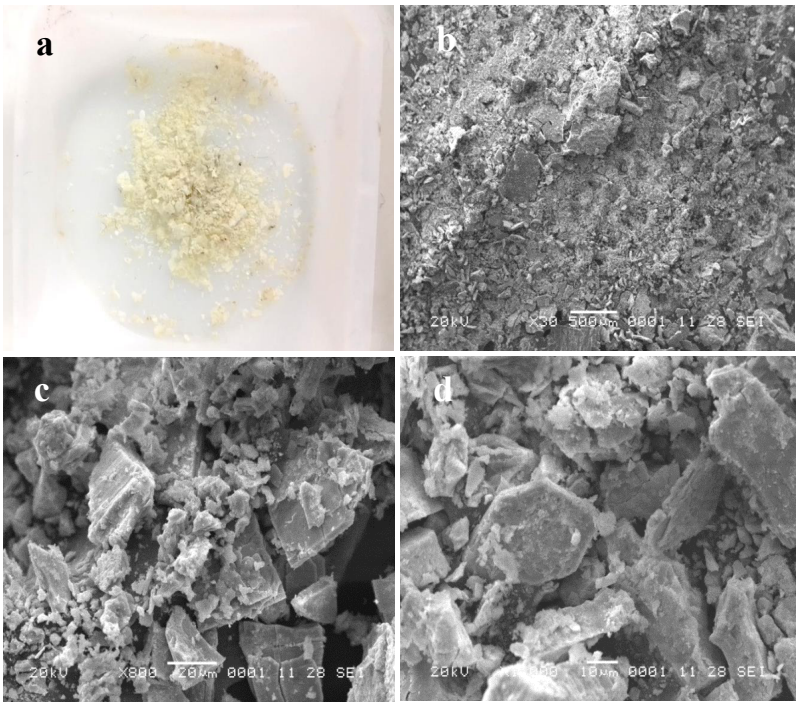

Figure 6. Magnification SEM images. a: Material recovered at the bottom of the cathodic chamber; b, c and d: Flaky crystals.

in Figures 5 and 6. Likewise, microcrystals (Needle-like structure) were observed from 2 to 5 μm wide such as the CeO_2 deposits obtained by electrochemical generation (Figures 5) (Zhou and Switzer, 1996; Zhou *et al*., 1995). Hachiya *et al*. (2009), synthesized cathodes to obtain sodium hydroxides by the chlor-alkali process, using a mixture of $RuCl_3$ and $CeCl_3$ supported on a Ni mesh, incinerated at 550 °C to obtain RuO_2 and CeO_2. The cathode electron micrographs show a similar morphology regarding Figure 5d; there were presence of microcrystals, using a cathode in an electrolytic cell, and it was similar to this work. Likewise, Hachiya found that the morphology of CeO_2 changes when applying current for a long time, obtaining needle-shaped crystals, due to the multiple superimposed layers (Figure 5d).

The material recovered at the bottom of the cathodic chamber had a flake-like appearance, characteristic of the precipitation of metallic species such as hydroxide (Figure 6), and which is not observed when recovering metallic species in their elemental form (Luo *et al*., 2014; Alcázar-Medina *et al*., 2020).

Conclusions

In this study, it was possible to obtain cerium oxides deposited on a stainless steel electrode and in the electrolyte using a cathode current of -2.5 Am^{-2} in a microbial electrochemical system operated under a highly saline electrolyte, and with a halotolerant bio-anode, where the energy demand is lower (0.6 to 1.2 V) when compared to the same system under abiotic conditions (1.9 V).

Acknowledgements

The authors thank the "Consejo Nacional de Ciencia y Tecnología" (CONACYT grant no. 421498) and CEMIE-Biogas-CONACYT-SENER (247006), in México, for the financial support. Likewise, the authors wish to thank Jorge Domínguez-Maldonado, Tanit Toledano Thompson, Eng., and Martin Baas, M.Sc., for technical assistance.

Nomenclature

MES & Microbial electrochemical systems
REEs & Rare earth elements
SHE & Standard hydrogen electrode
COD & Chemical oxygen demand
DSA & Dimensionally stable anodes
SCE & Standard calomel electrode
SEM & Scanning Electron Microscope
EDS & Energy Dispersive X-ray Spectrometer
XRD & X Ray diffraction

References

Alcázar-Medina, F.A., Núñez-Núñez, C.M., Villanueva-Fierro, I., Antileo, C., Proal-Nájera, J.B. (2020). Removal of heavy metals present in groundwater from a northern Mexico mining community using Agave tequilana Weber extracts. *Revista Mexicana de Ingeniería Química 19*, 1187-1199. https://doi.org/10.24275/rmiq/Bio1047.

Dehaine, Q., Filippov, L.O. (2015). Rare earth (La, Ce, Nd) and rare metals (Sn, Nb, W) as by-product of kaolin production, Cornwall: Part1: Selection and characterisation of the valuable stream. *Minerals Engineering 76*, 141-153. https://doi.org/10.1016/j.mineng.2014.10.006.

Fraggedakis, D., Bazant, M. Z. (2020). Tuning the stability of electrochemical interfaces by electron transfer reactions. *The Journal of Chemical Physics 152 (18)*, 184703. https://doi.org/10.1063/5.0006833.

Gaffney, E.M., Simoska, O., Minteer, S.D. (2021). The use of electroactive halophilic bacteria for improvements and advancements in environmental high saline biosensing. *Biosensors 11(2)*, 48. https://doi.org/10.3390/bios11020048.

Gómora-Hernández, J. C., Serment-Guerrero, J. H., Carreño-de-León, M. C., Flores-Alamo, N. (2020). Voltage Production in a plant microbial fuel cell using agapanthus africanus. *Revista Mexicana de Ingeniería Química 19(1)*, 227-237. https://doi.org/10.24275/rmiq/IA542.

Hachiya, T., Sasaki, T., Tsuchida, K., Houda, H. (2009). Ruthenium oxide cathodes for chlor-alkali electrolysis. *ECS Transactions 16*, 31. https://doi.org/10.1149/1.3104645.

Hua, T., Li, S., Li, F., Zhou, Q., Ondon, B. S. (2019). Microbial electrolysis cell as an emerging versatile technology: a review on its potential application, advance and challenge. *Journal of Chemical Technology & Biotechnology 94(6)*, 1697-1711. https://doi.org/10.1002/jctb.5898.

Jha, M.K., Kumari, A., Panda, R., Kumar, J.R., Yoo, K., Lee, J.Y. (2016). Review on hydrometallurgical recovery of rare earth metals. *Hydrometallurgy 165*, 2-26. https://doi.org/10.1016/j.hydromet.2016.01.035.

Jin, W., Zhang, Y. (2020). Sustainable electrochemical extraction of metal resources from waste streams: from removal to recovery. *ACS Sustainable Chemistry & Engineering 8(12)*, 4693-4707. https://doi.org/10.1021/acssuschemeng.9b07007.

Jordens, A., Cheng, Y.P., Waters, K.E. (2013). A review of the beneficiation of rare earth element bearing minerals. *Minerals Engineering 41*, 97-114. https://doi.org/10.1016/j.mineng.2012.10.017.

Kadier, A., Jain, P., Lai, B., Kalil, M.S., Kondaveeti, S., Alabbosh, K.F., Abu-Reesh, I., Mohanakrishna, G. (2020). Biorefinery perspectives of microbial electrolysis cells (MECs) for hydrogen and valuable chemicals production through wastewater treatment. *Biofuel Research Journal 7(1)*, 1128-1142. https://doi.org/10.18331/BRJ2020.7.1.5.

Kumar, P., Bharti, R.P. (2019). Nanocomposite polymer electrolyte membrane for high performance microbial fuel cell: Synthesis, characterization and application. *Journal of the Electrochemical Society 166(15)*, F1190. https://doi.org/10.1149/2.0671915jes/meta.

Luo, H.; Liu, G., Zhang, R., Bai, Y., Fu, S., Hou, Y. (2014). Heavy metal recovery combined with H_2 production from artificial acid mine drainage using the microbial electrolysis cell. *Journal of Hazardous Materials 270*, 153-159. https://doi.org/10.1016/j.jhazmat.2014.01.050.

Massari, S., Ruberti, M. (2013). Rare earth elements as critical raw materials: Focus on international markets and future strategies. *Resources Policy 38*, 36-43. https://doi.org/10.1016/j.resourpol.2012.07.001.

Modin, O., Wang, X., Wu, X., Rauch, S., Fedje, K.K. (2012). Bioelectrochemical recovery of Cu, Pb, Cd, and Zn from dilute solutions. *Journal of Hazardous Materials 235*, 291-297. https://doi.org/10.1016/j.jhazmat.2012.07.058.

Morrison, W.M., Tang, R. (2012). China's rare earth industry and export regime: economic and trade implications for the United States. Available at: https://fas.org/sgp/crs/row/R42510.pdf. Accessed: March 01, 2021.

Peeva, G., Yemendzhiev, H., Koleva, R., Nenov, V. (2020). Catalyst assisted microbial fuel cells. *Journal of Chemical Technology and Metallurgy 55(4)*, 824-830. https://dl.uctm.edu/journal/node/j2020-4/20_19-192_p_824-830.pdf.

Pikalova, E., Bogdanovich, N., Kolchugin, A., Ermakova, L., Khrustov, A., Farlenkov, A., Bronin, D. (2021). Methods to increase electrochemical activity of lanthanum nickelate-ferrite electrodes for intermediate and low temperature SOFCs. *International Journal of Hydrogen Energy*. https://doi.org/10.1016/j.ijhydene.2021.01.226.

Pozo, G., Pongy, S., Keller, J., Ledezma, P., Freguia, S. (2017). A novel bioelectrochemical system for chemical-free permanent treatment of acid mine drainage. *Water Research 126*, 411-420. https://doi.org/10.1016/j.watres.2017.09.058.

Prakash, G.K.S., Viva, F.A., Bretschger, O., Yang, B., El-Naggar, M., Nealson, K. (2010). Inoculation procedures and characterization of membrane electrode assemblies for microbial fuel cells. *Journal of Power Sources 195*, 111-117. https://doi.org/10.1016/j.jpowsour.2009.06.081.

Reimers, C.E., Girguis, P., Stecher, H.A., Tender, L.M., Ryckelynck, N., Whaling, P. (2006). Microbial fuel cell energy from an ocean cold seep. *Geobiology 4*, 123-136. https://doi.org/10.1111/j.1472-4669.2006.00071.x.

Reimers, C.E., Stecher, H.A., Westall, J.C., Alleau, Y., Howell, K.A., Soule, L., White, H.K., Girguis, P.R. (2007). Substrate degradation kinetics, microbial diversity, and current efficiency of microbial fuel cells supplied with marine plankton. *Applied Environmental Microbiology 73*, 7029-7040. https://doi.org/10.1128/AEM.01209-07.

Rimboud, M., Etcheverry, L., Barakat, M., Achouak, W., Bergel, A., Délia, M. L. (2021). Hypersaline microbial fuel cell equipped with an oxygen-reducing microbial cathode. *Bioresource Technology 337*, 125448. https://doi.org/10.1016/j.biortech.2021.125448.

Stamenkovic, V.R., Strmcnik, D., Lopes, P.P., Markovic, N.M. (2017). Energy and fuels from electrochemical interfaces. *Nature Materials 16*, 57-69. https://doi.org/10.1038/nmat4738.

Ter Heijne, A., Hamelers, H.V.M., De Wilde, V., Rozendal, R.A., Buisman, C.J.N. (2006). A bipolar membrane combined with ferric iron reduction as an efficient cathode system in microbial fuel cells. *Environmental Science and Technology 40*, 5200-5205. https://doi.org/10.1021/es0608545.

Torres, C.I., Krajmalnik-Brown, R., Parameswaran, P., Marcus, A.K., Wanger, G., Gorby, Y.A., Rittmann, B.E. (2009). Selecting anode-respiring bacteria based on anode potential: Phylogenetic, electrochemical, and microscopic characterization. *Environmental Science and Technology 43*, 9519-9524. https://doi.org/10.1021/es902165y.

Vanýsek, P. (2012). Electrochemical series. *Handbook of Chemical Physics 93*, 5-80. Available at: https://pdfs.semanticscholar.org/d69f/b8901fa978ef52cc489d4cac71bpd. Accessed: March 01, 2021.

Wang, Q., Huang, L., Pan, Y., Zhou, P., Quan, X., Logan, B.E., Chen, H. (2016). Cooperative cathode electrode and in situ deposited copper for subsequent enhanced Cd (II) removal and hydrogen evolution in bioelectrochemical systems. *Bioresource Technology 200*, 565-571. https://doi.org/10.1016/j.biortech.2015.10.084.

Xie, F., Zhang, T.A., Dreisinger, D., Doyle, F. (2014). A critical review on solvent extraction of rare earths from aqueous solutions. *Minerals Engineering 56*, 10-28. https://doi.org/10.1016/j.mineng.2013.10.021.

Zhang, Y., Angelidaki, I. (2014). Microbial electrolysis cells turning to be versatile technology: recent advances and future challenges. *Water Research 56*, 11-25. https://doi.org/10.1016/j.watres.2014.02.031.

Zhou, Y., Phillips, R.J., Switzer, J.A. (1995). Electrochemical synthesis and sintering of nanocrystalline cerium (IV) oxide powders. *Journal of the American Ceramic Society 78*, 981-985. https://doi.org/10.1111/j.1151-2916.1995.tb08425.x.

Zhou, Y., Switzer, J.A. (1996). Growth of cerium (IV) oxide films by the electrochemical generation of base method. *Journal of Alloys and Compounds 237*, 1-5. https://doi.org/10.1016/0925-8388(95)02048-9.

Zhu, X., Yates, M.D., Hatzell, M.C., Rao, H.A., Saikaly, P.E., Logan, B.E. (2014). Microbial community composition is unaffected by anode potential. *Environmental Science & Technology 48*, 1352-1358. https://doi.org/10.1021/es404690q.